Rapid determination of retinoic acid and its main isomers in plasma by second-order high-performance liquid chromatography data modeling

Carla M. Teglia, María S. Cámara & Héctor C. Goicoechea

Analytical and Bioanalytical Chemistry

ISSN 1618-2642
Volume 406
Number 30

Anal Bioanal Chem (2014)
406:7989-7998
DOI 10.1007/s00216-014-8268-8

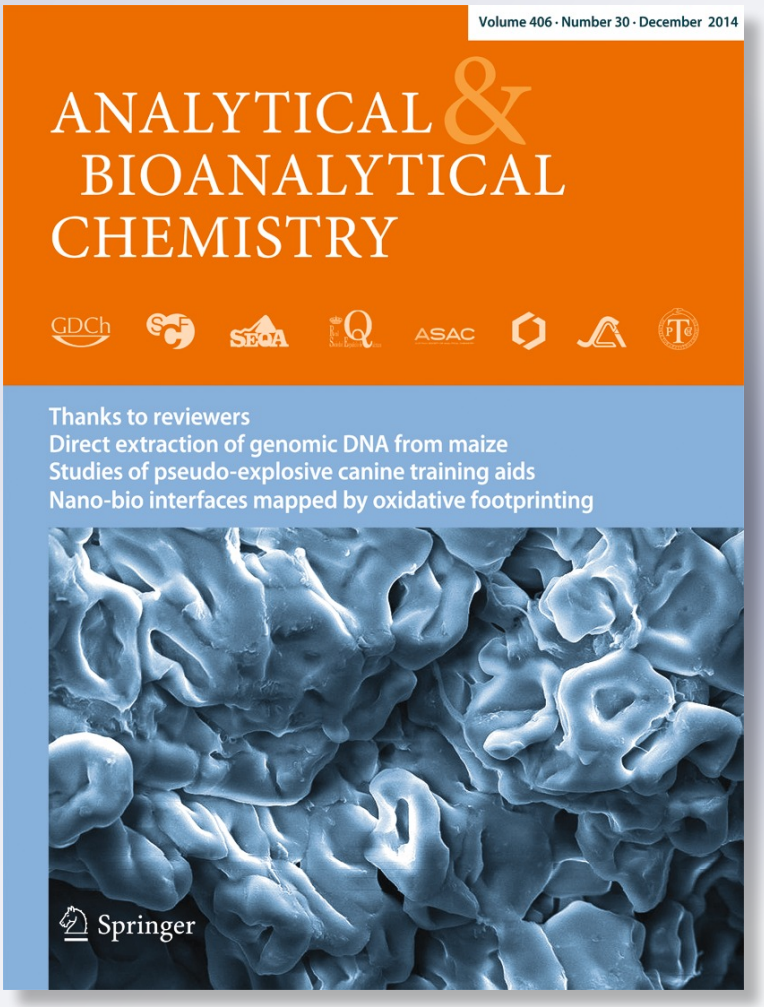

Springer

Anal Bioanal Chem (2014) 406:7989–7998
DOI 10.1007/s00216-014-8268-8

RESEARCH PAPER

Rapid determination of retinoic acid and its main isomers in plasma by second-order high-performance liquid chromatography data modeling

Carla M. Teglia · María S. Cámara · Héctor C. Goicoechea

Received: 14 July 2014 / Revised: 8 October 2014 / Accepted: 10 October 2014 / Published online: 5 November 2014

Abstract This paper reports the development of a method based on high-performance liquid chromatography (HPLC) coupled to second-order data modeling with multivariate curve resolution-alternating least-squares (MCR–ALS) for quantification of retinoic acid and its main isomers in plasma in only 5.5 min. The compounds retinoic acid (RA), 13-*cis*-retinoic acid, 9-*cis*-retinoic acid, and 9,13-di-*cis*-retinoic acid were partially separated by use of a Poroshell 120 EC–C18 (3.0 mm×30 mm, 2.7 μm particle size) column. Overlapping not only among the target analytes but also with the plasma interferents was resolved by exploiting the second-order advantage of the multi-way calibration. A validation study led to the following results: trueness with recoveries of 98.5–105.9 % for RA, 95.7–110.1 % for 13-*cis*-RA, 97.1–110.8 % for 9-*cis*-RA, and 99.5–110.9 % for 9,13-di-*cis*-RA; repeatability with RSD of 3.5–3.1 % for RA, 3.5–1.5 % for 13-*cis*-RA, 4.6–2.7 % for 9-*cis*-RA, and 5.2–2.7 % for 9,13-di-*cis*-RA (low and high levels); and intermediate precision (inter-day precision) with RSD of 3.8–3.0 % for RA, 2.9–2.4 % for 13-*cis*-RA, 3.6–3.2 % for 9,13-di-*cis*-RA, and 3.2–2.9 % for 9-*cis*-RA (low and high levels). In addition, a robustness study revealed the method was suitable for monitoring patients with dermatological diseases treated with pharmaceutical products containing RA and 13-*cis*-RA.

Keywords Endogenous compounds · Retinoic acid · Second-order calibration · Plasma

C. M. Teglia · M. S. Cámara · H. C. Goicoechea (✉)
Laboratorio de Desarrollo Analítico y Quimiometría (LADAQ), Cátedra de Química Analítica I, Facultad de Bioquímica y Ciencias Biológicas, Universidad Nacional del Litoral-CONICET, Ciudad Universitaria, 3000 Santa Fe, Argentina
e-mail: hgoico@fbcb.unl.edu.ar

Introduction

Retinoic acid is an active metabolite of vitamin A which coordinates several processes, for example cell proliferation and differentiation. Retinoic acid (RA) and related geometric isomers have been detected in blood and embryonic target cells of mammals and birds [1]. These compounds have been widely studied in birds and mammals. Imbalances of the compounds are associated with dysfunction, including a variety of dermal lesions, changes in secondary sexual characteristics, susceptibility to such diseases as cancer and parasitic infections, immunosuppression, inhibition of spermatogenesis, deformities, abnormal embryonic development, and a large number of other effects on reproduction [1]. Several endogenous geometric isomers of RA each has a unique function [2]. The presence of all-*trans*-RA, 9,13-*cis*-RA, 13-*cis*-RA, 9-*cis*-RA, and 11-*cis*-retinoids in different tissues and plasma has been reported [3].

Both RA and 13-*cis*-RA are widely used in the treatment of a variety of dermatological diseases, for example acne, psoriasis, skin cancer, and photo aging, and for regulating growth and differentiation of epithelial cells, sebum production, and collagen synthesis [2–4]. However, retinoid levels should be monitored owing to the teratogenicity of these compounds [5, 6].

Determination of RA requires chromatographic separation of endogenous isomers before detection [3], because the isomers of RA are isobaric and have similar ultraviolet (UV) spectral profiles. Thus, mass detection and/or single-wavelength UV detection cannot distinguish the identities of the geometric isomers that co-elute with RA. A literature search reveals that such techniques as gas chromatography (GC), high-performance liquid chromatography (HPLC) column-switching with and without direct injection of plasma, ultra-high-performance liquid chromatography (UHPLC),

and capillary electrophoresis (CE), with ultraviolet, fluorescence, and mass spectrometric detection have mostly been used to develop methods for quantification of RA and its isomers [7–11]. In most of these methods, the analytes were separated with retention times close to 30 min by use of C_{18} columns (4.6 mm×250 mm, 5.0 μm particle size) [6–9]. Very recently, an enhanced HPLC method in which the analytes were separated in 12 minutes by use of C_{18} (4.6 mm×75 mm, 3.5 μm particle size) has been developed in our laboratory [12].

Usually, full selectivity in chromatography enables separation and quantification of the analytes, despite the presence of interferences. When complete separation of the peaks cannot be achieved, generation of second-order data and its proper modeling by use of chemometric algorithms can guarantee selectivity by mathematical means, enabling resolution and quantification of coeluting analytes [13, 14]. It is well known that the information provided by second-order data, if adequately decomposed by use of suitable algorithms, can be uniquely ascribed to the analyte of interest, even in the presence of unexpected components not considered during calibration. This property has been called "the second-order advantage" and avoids the requirement for physical removal of interferences [15]. Two well-known second-order algorithms can be used to handle three-way arrays deviating from trilinearity (as usually occurs with HPLC–DAD data): multivariate curve resolution–alternating least-squares (MCR–ALS) [16] and parallel factor analysis 2 (PARAFAC2) [17]. They are able to take into account changes in shape and/or position of component profiles from sample to sample. When MCR–ALS is performed in the so-called extended mode, the challenge is overcome by building an augmented data matrix by appending calibration and test data matrices in the time direction, which is suspected of breaking the trilinear structure of the data. In this way, the rows represent spectra and the columns time profiles, alleviating the problems associated with sample-to-sample differences in this dimension [18]. PARAFAC2 is a variant of PARAFAC which allows for profile changes in one of the data modes, but requires fewer chemically natural constraints than MCR–ALS (non-negativity and unimodality). It is thus limited to similar changes in peak positions for different constituents in different samples.

Much work has been published on chemometric modeling of second-order data generated by HPLC. A search in Scopus using "HPLC" and "second-order data" as keys revealed that ca. 130 papers have been published since 1985, MCR–ALS being the algorithm of choice to solve most of the analytical problems reported [14, 19]. However, to the best of our knowledge, only two papers have reported the development of analytical methods for resolution and quantification of endogenous compounds in biological fluids; they report determination of pteridines in human urine [20, 21]. In this paper, we present a HPLC method with DAD coupled to the MCR–ALS algorithm to achieve the resolution and quantification of four analytes (retinoic acid and its isomers) in a complex mixture (plasma samples), in a shorter analysis time than reported previously. The method was thoroughly validated (which is rare in the development of multi-way calibration methods), and the results showed that the method can be conveniently adapted for monitoring patients with dermatological diseases treated with pharmaceutical products containing RA and 13-*cis*-RA.

Experimental

Apparatus, chromatographic conditions and software

All experiments were performed with an Agilent 1100 series liquid chromatograph equipped with a quaternary pump, degasser membrane, thermostated column compartment, autosampler, and diode-array detector (DAD) (Agilent Technologies, Waldbronn, Germany). The HPLC column was a Poroshell 120 EC–C18 (3.0 mm×30 mm, 2.7 μm particle size) from Agilent.

The chromatographic conditions were based on previous knowledge about the system [12]. In this work, however, the objective was to reduce the run time. Thus, the mobile phase (isocratic mode) was 76.5:1:22.5 methanol–acetonitrile–acidic aqueous solution (acetic acid 2 %+tetrahydrofuran 5 %). Column temperature was maintained at 30 °C and flow rate at 0.6 mL min^{-1}. Solutions and solvents used for mobile phase preparation were always filtered through 0.45-μm nylon filters. Standards and sample solutions were also filtered through 0.20 μm nylon syringe membranes before injection for chromatographic analysis.

Chromatograms for each sample were obtained in 5.5 min (path of 0.81 seg), and spectra were recorded from 200–500 nm (path of 2 nm). Region selection was then performed in the ranges 2.3–5.0 min and 240–442 nm, furnishing matrices of size 201×102 for each sample. This was to enable use of the most relevant information.

Chemstation version B 0103 was used for data acquisition and processing. All the algorithms were implemented in MATLAB 7.10 [22]. Those for applying MCR–ALS are available on the Internet at http://www.mcrals.info/.

Chemicals and reagents

RA (CAS 302–79–4) was purchased from Sigma (Sigma–Aldrich, St Louis, USA). Isotretinoin Roaccutan was purchased from Roche (R.P. Scherer, Eberbach, Germany). Hexane p.a. and ethyl acetate p.a. were supplied by Anedra (San Fernando, Argentina), and tetrahydrofuran p.a. and acetic acid p.a. by Cicarelli (San Lorenzo, Argentina). Acetonitrile and methanol, HPLC-grade, were obtained from Merck

(Darmstadt, Germany). HPLC-grade water was obtained from a Milli–Q Biocel System (Millipore, Molsheim, France).

Preparation of standard solutions and samples for the validation study

An RA stock standard solution of 0.500 mg mL^{-1} was prepared by exactly weighing and dissolving the appropriate amount of standard in methanol. The solution was stored at 4 °C in light-resistant containers and was allowed to reach room temperature before use.

During sample pretreatment (see the section "Sample preparation") RA standard is converted to a series of isomers in the proportions: 33.1 % RA, 35.6 % 13-*cis*-RA, 14.8 % 9-*cis*-RA, and 16.5 % 9,13-di-*cis*-RA. Another isomer is also formed (11-*cis*-RA), but not with significant percentage conversion (<1 %). Interestingly, this percentage conversion is maintained in every experiment. This was checked by performing the pretreatment on several standards solution (containing different initial RA concentrations). It was concluded that after 10 min percentage conversion remained constant. This enabled us to prepare standards for all four analytes (once the peaks were identified) from a single RA standard. Thus, calibration standard solutions were prepared at the moment of use by diluting an appropriate volume of the mentioned stock standard solution with methanol yielding concentrations in the ranges RA 0.25–7.55 μg mL^{-1}, 13-*cis*-RA 0.27–8.12 μg mL^{-1}, 9-*cis*-RA 0.11–3.37 μg mL^{-1} and 9,13-di-*cis*-RA 0.12–3.76 μg mL^{-1}. The different stock solutions (10 μL) were diluted with 40 μL blank human plasma to give concentrations of RA in the same ranges as for the methanolic solutions, to furnish standard solutions prepared in the sample matrix. All the standard solutions were processed in the same way as samples.

A solution of Isotretinoin Roaccutan 1.0 μg mL^{-1} was prepared by weighing and dissolving the drug in methanol; this was used to identify the peak of 13-*cis*-RA.

Sample preparation

The pretreatment recommended in Ref. [1] was followed. Sample plasma (50 μL) was transferred to a 1.5-mL centrifuge tube and 100 μL acetonitrile was added. The samples were vortex mixed for 10 s then 300 μL 1:1 ethyl acetate–hexane was added. Finally, the samples were vortex mixed for 10 s, centrifuged at 6000 rpm for 2 min, and the organic phase was transferred to glass tubes. The extraction was repeated three times and the combined organic phases were evaporated to dryness under a gentle stream of nitrogen gas. The residue was dissolved in 50 μL acetonitrile and 15 μL of the final solution was injected for HPLC analysis. Twenty five samples from different patients treated with 30–40 mg Isotretinoin Roaccutan per day were processed.

Method validation: limit of detection (LOD), limit of quantification (LOQ), linearity, precision, trueness, and robustness

LOD and LOQ were calculated by use of calibration curve data (univariate approach) and by application of the equations presented by Bauza et al. for quantitative analysis by use of MCR–ALS (multivariate approach) [23].

To study the linear range, calibration standards were prepared in triplicate in methanol at concentrations of 0.25, 0.67, 1.00, 2.52, 3.75, 4.99, 5.83, and 7.55 μg mL^{-1} (RA), 0.27, 0.72, 1.08, 2.71, 4.03, 5.37, 6.27, and 8.12 μg mL^{-1} (13-*cis*-RA), 0.11, 0.30, 0.45, 1.13, 1.68, 2.23, 2.60, and 3.37 μg mL^{-1} (9-*cis*-RA), and 0.11, 0.33, 0.50, 1.25, 1.87, 2.49, 2.90, and 3.76 μg mL^{-1} (9,13-di-*cis*-RA). These standard solutions were analyzed randomly. Finally, calibration plots were constructed by plotting peak area as a function of concentration for each analyte.

Repeatability was assessed by replicate analysis (n =10) of standard solutions at two different concentrations (LOQ and 100 % calibration curve), prepared by spiking blank human plasma with appropriately prepared standard solution. Intermediate precision was evaluated by replicate analysis of the same standard samples during three consecutive weeks. Relative standard deviation (RSD, %) was calculated in both precision studies.

Recovery was assessed by replicate analysis (n =3) of spiked samples at five different concentrations (RA: 0.76, 1.82, 3.60, 5.49 and 6.44 μg mL^{-1}; 13-*cis*-RA: 0.82, 1.96, 3.89, 5.93 and 6.95 μg mL^{-1}; 9-*cis*-RA: 0.34, 0.82, 1.62, 2.47 and 2.90 μg mL^{-1}; 9,13-di-*cis*-RA: 0.38, 0.91, 1.80, 2.75 and 3.22 μg mL^{-1}), prepared by spiking blank human plasma with a convenient volume of standard solution. The following assays were then performed:

1. linearity of nominal concentrations as a function of peak area was studied for each analyte;
2. the slopes obtained were compared with those corresponding to calibration curves with pure analyte in solvent;
3. nominal concentrations were plotted as a function of predicted concentration and the elliptic joint confidence region (EJCR) test [24] was applied for each analyte to evaluate the slopes and intercepts; and
4. recoveries were computed.

In addition, twenty-five real samples from patients treated with Isotretionin Roaccutan were analyzed by use of an HPLC method involving total separation of the analytes and plasma components, which was used as a "reference method" [12]. Subsequently, concentrations provided by both methods were computed and compared by use of the EJCR test.

To assess method robustness, different chromatographic conditions were varied within a realistic range and the effect of these changes on the number of peaks, analysis time, and the quality of the modeling were evaluated. A twelve-experiment Plackett–Burman (PB) [25] design was constructed considering small variations percent MeOH (76–77 %), acetonitrile (0.5–1.5 %), and the acid aqueous solution (the amount necessary to reach 100 %), flow rate (0.55–0.65 mL min^{-1}), and column temperature (29–31 °C). The design was built with Design Expert software (Design Expert 8.0.5, 2010; Stat-Ease, Minneapolis, USA); twelve is the smallest number of experiments that can be conducted using this software.

Results and discussion

Development of a chromatographic method involving complete separation of RA and its main isomers was reported very recently by our group [12]. In this work, the total chromatographic run takes ca 12 min, a substantial reduction of time, and, consequently, of amount of waste solvents, compared with previously reported methods (see below). The separation was achieved by using chromatographic conditions optimized by application of response surface methodology [12]. However, in the current work, these conditions were modified to achieve the main objective: reduction of the time by half, even in presence of overlapping peaks, and mathematical resolution by use of three-way modeling. Figure 1 shows the chromatogram recorded for a plasma sample containing RA: 4.993 μg mL^{-1}, 13-*cis*-RA: 5.37 μg mL^{-1}, 9-*cis*-RA: 2.23 μg mL^{-1}, and 9,13-di-*cis*-RA: 2.49 μg mL^{-1}. It corresponds to a second-order data matrix obtained by recording spectra as a function of elution time. As can be appreciated, substantial overlapping of the four analytes and plasma components is evident in the region 2.8–4.6 min, because of partial separation of the analytes and plasma components.

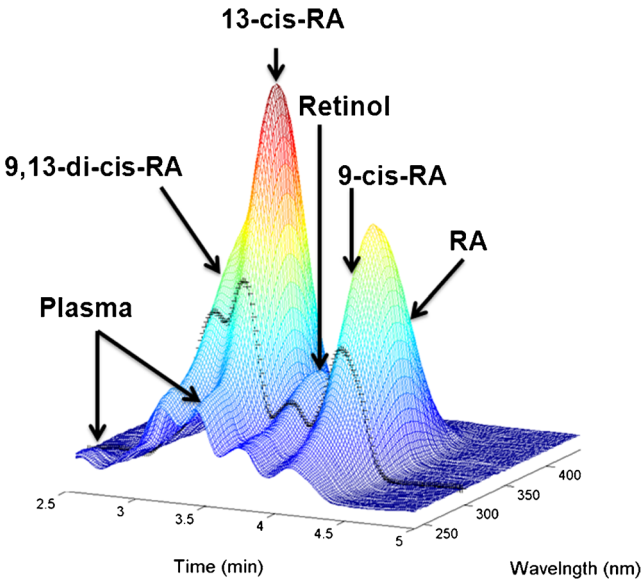

Fig. 1 Landscape showing the second-order data corresponding to a plasma sample spiked with a standard solution to reach concentrations of: RA 4.993 μg mL^{-1}, 13-*cis*-RA 5.37 μg mL^{-1}, 9-*cis*-RA 2.23 μg mL^{-1}, and 9,13-di-*cis*-RA 2.49 μg mL^{-1}. The *black cross line* corresponds to the chromatogram recorded at 280 nm. Conditions: methanol 76.5 %+acetonitrile 1.0 %+acid aqueous solution 22.5 %, column temperature 30 °C, and flow rate 0.6 mL min^{-1}

MCR–ALS analysis

MCR–ALS is an algorithm capable of handling data sets deviating from trilinearity, i.e., data in which changes of analyte migration time or peak shape occur from sample to sample [14]. With this purpose, the strategy of augmenting matrices along the mode which is suspected of breaking the trilinear structure is implemented. Thus, if matrix-to-matrix variation of profiles occurs along the column direction, a column-wise augmented matrix is created. Bilinear decomposition of the augmented matrix $\mathbf{D}_{aug}$ is performed by use of the expression:

$$\mathbf{D}_{aug} = \mathbf{C}_{aug} \times \mathbf{S}^{T} + \mathbf{E}_{aug} \quad (1)$$

in which the rows of $\mathbf{D}_{aug}$ contain the UV–visible spectra (K wavelengths) as a function of time (J times), the columns of $\mathbf{C}_{aug}$ contain the time profiles of the N compounds involved in the process, the columns of $\mathbf{S}$ their related spectra, and $\mathbf{E}_{aug}$ is a matrix of residuals not fitted by the model. Decomposition of $\mathbf{D}_{aug}$ is achieved by iterative least-squares minimization of $||\mathbf{E}_{aug}||$, under suitable constraining conditions, i.e., non-negativity of the spectral profiles, unimodality and non-negativity of the time profiles, and correspondence among species and samples for samples containing unexpected constituents. The building of $\mathbf{D}_{aug}$ can be viewed as starting from the individual data matrices for a number of samples, by placing them adjacent to each other, along the mode of the varying constituent profiles. Although the pure spectrum of each compound should be the same in all experiments and the spectral mode must be selective, the temporal profiles in the different $\mathbf{C}$ sub-matrices need not share a common shape. This is the reason chromatographic runs can be analyzed together even in the presence of elution time shifts from sample to sample, i.e. non-trilinear data. Thus, the first modeling step consisted in building an augmented data matrix $\mathbf{D}_{aug}$ in the temporal mode by stacking the data matrices corresponding to each validation or test sample followed by those of the standard samples for each analyte. Consequently, the dimension of the each built augmented matrix is (5025 × 102), where 5025 is the product of 25 (24 standard samples—eight levels in triplicate—plus one being analyzed) and 201 (number of

chromatographic time points), and 102 is the number of digitized wavelengths.

As is well known, MCR–ALS requires initialization with system properties as close as possible to the final results. Thus, analyte and interference spectra are required, because the resolution is based on selectivity in the spectral mode. In this work, the latter were obtained by selection of the purest spectra, by using routines written in this laboratory [26].

The number of contributing species in the system under study, when applying singular value decomposition (SVD) was always equal to the real number of components, i.e. four when analyzing standard samples (see the comments above), but two more components should be considered when analyzing plasma samples: one unknown plasma component and one peak corresponding to retinol. Figure 2a shows the retrieved chromatograms for all six mentioned components, and Fig. 2b shows the corresponding spectra. As can be appreciated, severe overlapping occurs, especially in the spectra corresponding to RA and 13-*cis*-RA, although the MCR–ALS modeling enabled us to obtain acceptable results (see below).

After MCR–ALS decomposition of $\mathbf{D}_{aug}$, concentration information of standard samples contained in $\mathbf{C}_{aug}$ (the areas under the temporal profiles of each component) was used to construct the univariate regression of areas against analyte concentrations.

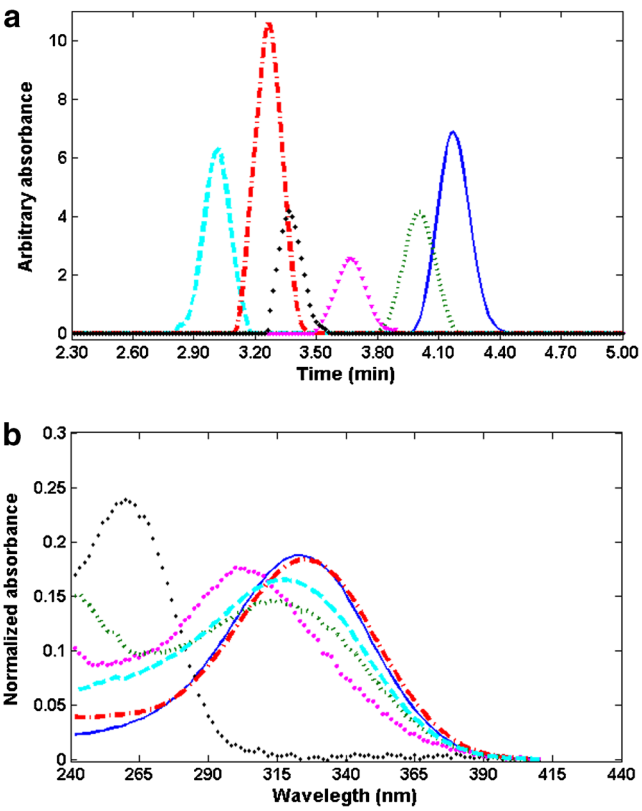

Fig. 2 (**a**) Concentration profiles retrieved by MCR–ALS for a plasma sample containing 9,13-di-*cis*-RA (*sky-blue dashed line*), 13-*cis*-RA (*red dash–dotted line*), retinol (*magenta triangles*), 9-*cis*-RA (*green dots*), RA (*blue solid line*), and plasma interferent (*black diamond*). (**b**) Spectral profiles retrieved by MCR–ALS for the same sample as in **a**

In addition, the degree of rotational ambiguity was evaluated to perform evaluation of the quality of the MCR–ALS modeling. This was done to determine whether the solutions provided by the decomposition are practically unique. For this purpose, the software presented by Jaumot and Tauler was used (http://www.cid.csic.es/homes/rtaqam/tmp/WEB_MCR/welcome.htm) [27]. In this context, the profiles for RA, 13-*cis*-RA, 9-*cis*-RA, and 9,13-di-*cis*-RA were retrieved, giving the maximum and minimum values for a function which gives the relative signal contribution of a particular component to the whole signal for the mixture of N components:

$$f_{\mathrm{n}} = \frac{\left\|\mathbf{c}_n \mathbf{s}_n^{\mathrm{T}}\right\|}{\left\|\mathbf{C}\mathbf{S}^{\mathrm{T}}\right\|} \tag{2}$$

where f_{n} is a scalar value and $\|.\|$ is the Frobenious norm. Modeling was performed implementing the three constraints normalization, non-negativity, and unimodality. It showed that profiles do not change during the optimization. This conclusion is reached by analyzing the relationships between $f_{\max}$ and $f_{\min}$, which should be nearest to zero (more details are given in Ref. [27]). The results obtained are listed in Table 1.

Validation results

Linear range

Calibration curves were obtained by triplicate analysis of eight standard mixtures covering the whole linear range. Curves plotted using areas from profiles retrieved by MCR–ALS revealed a good linear relationship (r^2>0.9999) between 0.25 and 7.55 μg mL^{-1} for RA; 0.27 and 8.14 μg mL^{-1} for 13-*cis*-RA; 0.11 and 3.40 μg mL^{-1} for 9-*cis*-RA; 0.11, and 3.79 μg mL^{-1} for 9,13-di-*cis*-RA; the calibration data are listed in Table 2. However, for assessment of the linearity of an analytical method, linear regression calculations are not sufficient and,

Table 1 Effect of constraints on rotational ambiguity for all components

$f^{\max} - f^{\min}$	Constraints		
	1 and 2	1, 2, and 3	1, 2, 3, and 4
RA	0.488	0.007	−0.005
13-*cis*-RA	0.471	0.005	0.082
9-*cis*-RA	0.133	−0.032	0.151
9,13-di-*cis*-RA	0.351	0.049	0.260

Constraints: 1 normalization; 2 non-negativity; 3 unimodality; 4 trilinearity

$f^{\max} - f^{\min}$: corresponds to the difference between $f^{\max}$ and $f^{\min}$ values [27]

Table 2 Linear ranges and analytical figures of merit

Variable	Experimental value[a]			
	RA	13-*cis*-RA	9-*cis*-RA	9,13-di-*cis*-RA
Linear range (μg mL^{-1})	0.25–7.55	0.27–8.12	0.11–3.370	0.12–3.76
Intercept	−133.6 (6.0)	−1.6 (7.4)	77.3 (7.6)	6.6 (3.1)
Slope	571.3 (1.4)	578.6 (1.6)	535.9 (4.0)	512.0 (−3.1)
F_{exp} [b]	2.25	2.20	1.56	2.23
r^2	0.9999	0.9999	0.9994	0.9999
Lack of fit (*p*-value)[c]	0.113	0.114	0.339	0.144

[a] Values between parentheses indicate standard deviation

[b] F_{tab} =3.80

[c] Because the *p*-value for the lack of adjustment is greater than or equal to 0.10, the model seems to be adequate for the observed data

therefore, the goodness of fit was tested by comparing the variance of the lack of fit against the pure error variance, as published by several authors [28–31]. The adequacy of the model was estimated by use of a *F*–test (Table 2).

Homoscedasticity was checked by applying the Levene test (for each analyte); this revealed no significant difference between variances of the different standard concentrations ($p > 0.05$), indicating homoscedasticity of the data. Homoscedasticity was also checked by calculating the residual values as the differences between the actual value and that predicted from the regression curve, and plotting these against the actual concentration of calibration standards. Homoscedasticity was confirmed, because residual values were randomly distributed about the regression line without any trend [32].

Limits of detection (LOD) and quantification (LOQ)

Different approaches are available for computing LOD and LOQ [33, 34]. In this work they were computed from the linear regression analysis by using the standard deviation of the regression (S_y), by use of the expressions [33]:

$$\mathrm{LOD} = \frac{3.3\,S_y}{b} \tag{3}$$

and

$$\mathrm{LOQ} = \frac{10\,S_y}{b} \tag{4}$$

The values obtained are reported in Table 3.

In addition, according to Bauza et al. [23], sensitivity (SEN) when MCR–ALS is applied can be estimated by use of Eq. 5:

$$\mathrm{SEN}_{\mathrm{MCR}} = m_n \left[J \left(\mathbf{S}^T \mathbf{S} \right)^{-1}_{nn} \right]^{-1/2} \tag{5}$$

in which *n* is the index for the analyte of interest in a multicomponent mixture, m_n is the slope of the MCR univariate calibration graph for this analyte, $\mathbf{S}^T$ is a matrix containing the profiles for all the sample components in the nonaugmented MCR direction (Eq. 1), and *J* is the number of channels in the test sample data matrix in the augmented MCR direction. The values obtained are reported in Table 3, and, as can be appreciated, the multivariate approach furnishes slightly higher values of the computed figures of merit.

Interestingly, the quantification limits and the linear range achieved by use of this methodology, are enough to measure the levels of RA and 13-*cis*-RA for patients treated with Isotretinoin Roaccutan, which are in the range 0.2–1.0 μg mL^{-1}, as was shown by bioequivalence studies [8].

Precision

In accordance with the recommendations of Refs. [35, 36], two conditions were studied: repeatability (or intra-assay) and intermediate variations (or inter-assay), with analysis of the four analytes being performed during three consecutive weeks using samples prepared as described in the section "Method validation: limit of detection (LOD), limit of quantitation (LOQ), linearity, precision, trueness and robustness". The figures of merit were calculated as the RSD (%); the values obtained are listed in Table 4. From this study it can be concluded that the precision of the method is excellent,

Table 3 LOD and LOQ values

Criteria	Parameter	Experimental value (μg mL^{-1})			
		RA	13-*cis*-RA	9-*cis*-RA	9,13-di-*cis*-RA
Calibration curve	LOD	0.071	0.086	0.037	0.041
	LOQ	0.207	0.251	0.108	0.119
MCR–ALS	LOD	0.080	0.090	0.041	0.056
	LOQ	0.240	0.273	0.125	0.169

Table 4 Results obtained in the precision study

Variable	Experimental value for low (L) and high (H) levels							
	RA		13-*cis*-RA		9-*cis*-RA		9,13-RA	
	L	H	L	H	L	H	L	H
Intra–assay precision RSD (%)[a]	3.5	3.1	3.5	1.5	4.6	2.7	5.2	2.7
Inter–assay precision RSD (%)[a]	3.8	3.0	2.9	2.4	3.2	2.9	3.6	3.2
p–value[b]	0.353	0.261	0.186	0.499	0.258	0.825	0.072	0.223

[a] Acceptable criterion: RSD ±20 %

[b] Because the *p*-value is greater than or equal to 0.05, there is no statistically significant difference between the mean values

considering that for bioanalysis acceptable RSD values are ≤15 % [37].

For further evaluation of inter-assay precision, analysis of variance was determined for the recoveries obtained for each concentration level during the three weeks, in such a way that both within-condition and between-condition variances were taken into account (Table 4). The *p*-values obtained, which were >0.05, enabled us to conclude there were no significant differences between the mean recoveries for each level in the three different weeks studied, with a confidence level of 0.05 for each analyte. Moreover, homoscedasticity was checked by applying the Bartlett statistic test; this revealed no significant difference between variances for the different standard concentrations (p >0.05), indicating homoscedasticity of the data [38].

Trueness

Because no certified reference materials were available, recovery was evaluated by spiking blank human plasma with known amounts of standard solutions at the beginning of the sample-preparation procedure, as recommended by Schmidt et al. [35]. After extraction and analysis, the response for blank human plasma was subtracted from the response for the spiked plasma sample, and recoveries were then calculated by interpolation of these new responses on the calibration graph.

Five levels were evaluated (three replicates) to construct calibration curves for matrix spiked with each analyte, with the object of comparing the slopes obtained for calibration curves prepared for methanol (pure analyte in solvent). This study showed the existence of linearity, and comparison of slopes computed in both situations were not statically different, indicating the absence of matrix effects.

Nominal concentrations vs. predicted values were then compared by use of an elliptic joint confidence region test. As can be clearly seen in the inset of Fig. 3a, the elliptical domains obtained for all the four analytes contain the theoretically predicted value of the slope (1) and the intercept (0); this is indicative of the absence of bias.

Finally, results obtained by use of both this method and the "reference" method for analysis of twenty-five real samples were also compared by use of the EJCR test. In this case, it should be remarked that the analyte 9-*cis*-RA could not be accurately quantified by use of the "reference method" owing to overlap of its peak with that of ROH. Thus, only three ellipses contain the theoretically predicted value of the slope (1) and intercept (0) (Fig. 3b); this was not observed for the region corresponding to 9-*cis*-RA. These observations

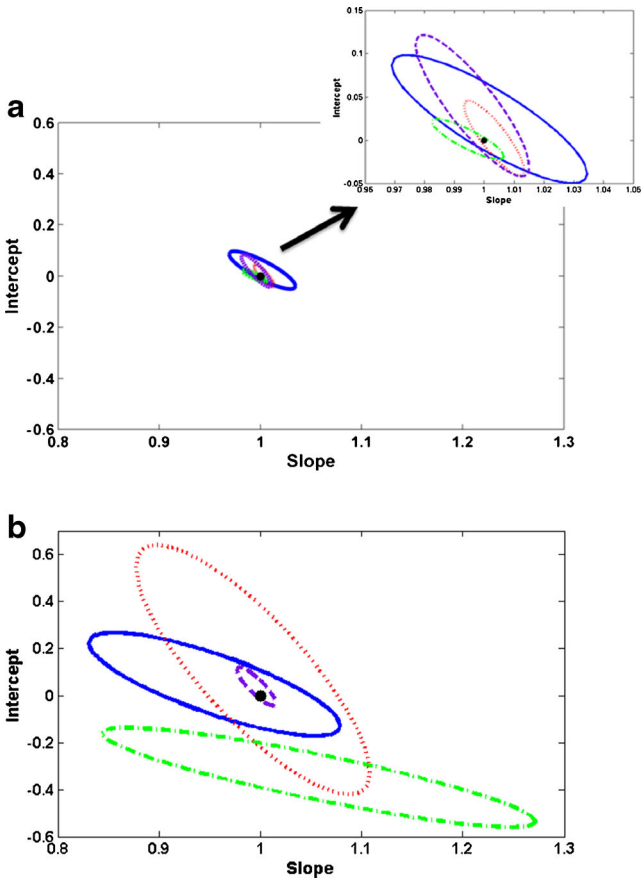

Fig. 3 Elliptic joint confidence region (EJCR) test for: (**a**) the predicted results for the fifteen spiked samples (five levels in triplicate) when plotting nominal vs. predicted values, and (**b**) the predicted results for the twenty-five plasma samples when plotting predicted values obtained with the reference method vs. those predicted by use of the novel method. 9,13-*cis*: *blue solid line*, 13-*cis*: *red dots*, 9-*cis*: *green dash–dotted line*, and RA: *violet dashed line*

indicate that both methods provide comparable results for RA, 13-*cis*-RA, and 9,13-*cis*-RA. Interestingly, the new method provides better results than the total separation HPLC method because the former enables quantification of 9-*cis*-RA. It is also apparent from the size of the elliptic regions in Fig. 3a, b that, as expected, more precision was obtained when analyzing validation samples than when analyzing real samples, although results from replicate analysis of the latter, with RSD% values <5, enable us to conclude the performance of the method is excellent.

Robustness

After conducting the experiments suggested by the PB experimental design, the number of peaks and the end time were obtained as responses from the chromatograms. Then, an ANOVA test was applied to the experimental data using the effects of dummy variables to obtain estimates of standard errors, to evaluate the effect of the experimental variations on the responses. The statistical test showed that small variations in the four factors have significant effect on end time, although the number of peaks (4) does not change. However, besides the effect on analysis time, the analyte profiles could be correctly retrieved in the twelve experiments, and quantified with acceptable accuracy by using standards which were run under similar conditions. This enabled us to conclude the method is robust.

Analysis of real samples

Analysis of the levels of the target biomarkers in the 25 samples analyzed, from patients treated with Isotretinoin Roaccutan, revealed the predominant species were: 13-*cis*-RA (35.8–53.4 %), RA (23.2–43.4 %), 9,13-di-*cis*-RA (10.2–20.1 %), and 9-*cis*-RA (2.6–13 %). This finding is consistent with the fact that the active ingredient of the pharmaceutical (13-*cis*-RA) follows the RA pathway (RA joint their receptors, enabling genetic transcription in the target cells [5]), and that a high level of 13-*cis*-RA should be maintained to avoid other processes. It should also be remarked that the concentrations of 13-*cis*-RA measured in this work ranged between 0.2 and 1.3 μg mL^{-1}. These levels agree well with those reported by Wu et al. in a bioequivalence study in which a method based on high-performance liquid chromatography–electrospray ionization mass spectrometry was used for quantification of isotretinoin in human plasma [8]. This confirms the suitability of this environmentally benign method, which is simpler than others reported previously, for monitoring patients being treated with Isotretinoin Roaccutan.

Comparison with published work

Comparison with other methods published in the literature was conducted to show the advantages of the method reported

Table 5 Comparison with other literature methods for determination of RA

Technique	Characteristics	Figures of merit (μg mL^{-1})	Time (min)	Ref.
HPLC UV–visible	Column: Inertsil C18 (4.6 mm×250 mm, 5 μm) Extraction: liquid–liquid	Linear range: 0.050–5.000 LOD: 0.020 (calibration curve) LOQ: 0.050 (calibration curve)	25	[1]
CE UV–visible	Capillary: fused–silica 50 μm ID, 8.5 cm outlet and 56 cm Extraction: none Direct injection	Linear range: 0.20–30.0 LOD: 0.060 (S/R) LOQ: 0.200 (S/R)	10	[7]
HPLC UV–visible	Column: Inertsil C18 (4.6 mm×250 mm, 5 μm) Extraction: liquid–liquid	Linear range: 0.003–0.600 LOQ: 0.001 (calibration curve) LOQ: 0.003 (calibration curve)	60	[9]
HPLC UV–visible	Column: LiChroCART HPLC C18 (4.0 mm×250 mm, 5 μm) Extraction: liquid–liquid	Linear range: 0.0003–0.100 LOD: 0.0009 (S/R) LOQ: 0.0003 (S/R)	35	[10]
HPLC UV–visible	Column Switching System Column: LiChroCART HPLC C18 (4.0 mm×125 mm and 4.0 mm×250 mm) Extraction: liquid–liquid	Linear range: 0.003–2.000 LOD: 0.001 (S/R) LOQ: 0.003 (S/R)	30	[11]
HPLC UV–visible	Column: Zorbax C18 (4.6 mm×75 mm, 3.5 μm) Extraction: liquid–liquid	Linear range 0.005–4.900 LOD: 0.002 (Eurachem) LOQ: 0.005 (Eurachem)	12	[12]
HPLC DAD MCR–ALS	Column: Poroshell 120 EC–C18 (3.0×30 mm, 2.7 μm particle size) Second-order data modeled with MCR–ALS algorithm	Linear range 0.200–7.500 LOD: 0.070 (univariate approach) LOQ: 0.210 (univariate approach) LOD: 0.080 (multivariate approach) LOQ: 0.240 (multivariate approach)	5.5	This work

Eurachem (Ref. [34])

in this paper. Different approaches, their main characteristics, and their figures of merit are listed in Table 5. It is apparent that one important achievement is reduction of analysis time. When HPLC–UV–visible methods are compared, the time saving is substantial. Comparison with our previously published work reveals run time is reduced by 50 %, although the LOQ is substantially (fiftyfold) higher. This is because the mobile phase conditions are different. However, it should be remarked that the LOQ achieved by use of this method is low enough for monitoring of the drug and its metabolites in patients treated with Isotretinoin Roaccutan. When the new method is compared with a CE-based method, the analysis time is also reduced, by ca 40 %, with the LOD being similar for both methods, i.e. sensitivity is maintained by implementation of the new method when the fastest methods are compared.

Conclusions

Quantification of RA and its main isomers in plasma could be performed for patients treated with Isotretinoin Roaccutan, a pharmaceutical used for the treatment of skin disorders. Determination of four analytes in the presence of unexpected compounds can be performed by using second-order data generated by use of HPLC coupled to DAD. The method was validated for all four analytes. Performance was excellent in terms of trueness and precision. In addition, a robustness study showed that the analytes can be correctly quantified even in presence of small variations of the main factors affecting the chromatographic procedure.

Plasma samples containing the analytes and interferents can be analyzed in 5.5 min only, an improvement on previously reported methods. By use of this method, amounts of solvents used in the separation step are reduced, which is highly recommended by the principles of green analytical chemistry [31].

Acknowledgments The authors are grateful to Universidad Nacional del Litoral (projects CAI+D 2011 nos 11-25 and 11-11), to CONICET (Consejo Nacional de Investigaciones Científicas y Técnicas, Project PIP 2012-14 no. 455), and to ANPCyT (Agencia Nacional de Promoción Científica y Tecnológica, Project PICT 2011-0005) for financial support. C.M.T. thanks CONICET for her fellowship.

References

1. Bérubé VE, Boily MH, DeBlois C, Dassylva N, Spear PA (2005) Plasma retinoid profile in bullfrogs, Rana catesbeiana, in relation to agricultural intensity of sub-watersheds in the Yamaska River drainage basin, Québec, Canada. Aquat Toxicol 71:109–120. doi:10.1016/j.aquatox.2004.10.018
2. Ioele G, Cione E, Risoli A, Genchi G, Ragno G (2005) Accelerated photostability study of tretinoin and isotretinoin in liposome formulations. Int J Pharm 293:251–260. doi:10.1016/j.ijpharm.2005.01.012
3. Kane MA (2012) Analysis, occurrence, and function of 9-*cis*-retinoic acid. BBA-Mol Cell Bioll 1821:10–20. doi:10.1016/j.bbalip.2011.09.012
4. Ourique AF, Melero A, de Bona da Silva C, Schaefer UF, Pohlmann AR, Guterres SS, Lehr CM, Kostka KH, Beck RC (2011) Improved photostability and reduced skin permeation of tretinoin: development of a semisolid nanomedicine. Eur J Pharm Biopharm 79:95–101. doi:10.1016/j.ejpb.2011.03.008
5. Das BC, Thapa P, Karki R, Das S, Mahapatra S, Liu T-C, Torregroza I, Wallace DP, Kambhampati S, Van Veldhuizen P, Verma A, Ray SK, Evans T (2014) Retinoic acid signaling pathways in development and diseases. Bioorg Med Chem 22:673–683. doi:10.1016/j.bmc.2013.11.025
6. Thibodeau J, Filion S, Spear P, Paquin J, Boily M (2012) Oxidation of retinoic acids in hepatic microsomes of wild bullfrogs Lithobates catesbeianus environmentally-exposed to a gradient of agricultural contamination. Ecotoxicology 21:1358–1370. doi:10.1007/s10646-012-0889-0
7. El-Hady DA, Albishri HM (2012) Hyphenated affinity capillary electrophoresis with a high-sensitivity cell for the simultaneous binding study of retinol and retinoic acid in nanomolars with serum albumins. J Chromatogr B 911:180–185. doi:10.1016/j.jchromb.2012.11.007
8. Wu C, Njar V, Brodie A, Borenstein M, Nnane I (2004) Quantification of a novel retinoic acid metabolism inhibitor, 4-(1H-imidazol-1-yl)retinoic acid (VN/14-1RA) and other retinoids in rat plasma by liquid chromatography with diode-array detection. J Chromatogr B 810:203–208. doi:10.1016/j.jchromb.2004.07.028
9. Miyagi M, Yokoyama H, Shiraishi H, Matsumoto M, Ishii H (2001) Simultaneous quantification of retinol, retinal, and retinoic acid isomers by high-performance liquid chromatography with a simple gradiation. J Chromatogr Biomed 757:365–368. doi:10.1016/S0378-4347(01)00158-X
10. Wyss R, Bucheli F (1997) Determination of endogenous levels of 13-*cis*-retinoic acid (isotretinoin), all-trans-retinoic acid (tretinoin) and their 4-oxo metabolites in human and animal plasma by high-performance liquid chromatography with automated column switching and ultraviolet detection. J Chromatogr Biomed 700:31–47. doi:10.1016/S0378-4347(97)00303-4
11. Hartmann S, Froescheis O, Ringenbach F, Wyss R, Bucheli F, Bischof S, Bausch J, Wiegand UW (2001) Determination of retinol and retinyl esters in human plasma by high-performance liquid chromatography with automated column switching and ultraviolet detection. J Chromatogr Biomed 751:265–275. doi:10.1016/S0378-4347(00)00481-3
12. Teglia CM, Gil García MD, Galera MM, Goicoechea HC (2014) Enhanced high-performance liquid chromatography method for the determination of retinoic acid in plasma. Development, optimization and validation. J Chromatogr A 1353:40–48. doi:10.1016/j.chroma.2014.01.013
13. Escandar GM, Olivieri AC, Faber NM, Goicoechea HC, Muñoz de la Peña A, Poppi RJ (2007) Second- and third-order multivariate calibration: data, algorithms and applications. TrAC Trends Anal Chem 26:752–765. doi:10.1016/j.trac.2007.04.006
14. Escandar GM, Goicoechea HC, Muñoz de la Peña A, Olivieri AC (2014) Second- and higher-order data generation and calibration: A tutorial. Anal Chim Acta 806:8–26. doi:10.1016/j.aca.2013.11.009
15. Booksh KS, Kowalski BR (1994) Theory of Analytical Chemistry. Anal Chem 66:782A–791A. doi:10.1021/ac00087a718
16. Tauler R (1995) Multivariate curve resolution applied to second order data. Chemometr Intell Lab 30:133–146. doi:10.1016/0169-7439(95)00047-X

17. Bro R (1998) Doctoral Thesis. University of Amsterdam, The Netherlands
18. Tauler R, Maeder M, de Juan A (2009) 2.24 - Multiset Data Analysis: Extended Multivariate Curve Resolution. In: Brown SD, Tauler R, Walczak B (eds) Comprehensive Chemometrics. Elsevier, Oxford, pp 473–505. doi:10.1016/B978-044452701-1.00055-7
19. Goicoechea HC, Culzoni MJ, García MDG, Galera MM (2011) Chemometric strategies for enhancing the chromatographic methodologies with second-order data analysis of compounds when peaks are overlapped. Talanta 83:1098–1107. doi:10.1016/j.talanta.2010.07.057
20. Llanos AM, Zan MM, Culzoni MJ, Espinosa-Mansilla A, Cañada-Cañada F, Peña AM, Goicoechea HC (2011) Determination of marker pteridines in urine by HPLC with fluorimetric detection and second-order multivariate calibration using MCR–ALS. Anal Bioanal Chem 399:2123–2135. doi:10.1007/s00216-010-4071-3
21. Culzoni MJ, Mancha de Llanos A, De Zan MM, Espinosa-Mansilla A, Cañada-Cañada F, Muñoz de la Peña A, Goicoechea HC (2011) Enhanced MCR–ALS modeling of HPLC with fast scan fluorimetric detection second-order data for quantification of metabolic disorder marker pteridines in urine. Talanta 85:2368–2374. doi:10.1016/j.talanta.2011.07.086
22. MATLAB (2010) Matlab 7.10. The Math Works Inc. Natick Massachusetts
23. Bauza MC, Ibañez GA, Tauler R, Olivieri AC (2012) Sensitivity Equation for Quantitative Analysis with Multivariate Curve Resolution-Alternating Least-Squares: Theoretical and Experimental Approach. Anal Chem 84:8697–8706. doi:10.1021/ac3019284
24. Jordi R, Rius FX (1997) Method comparison using regression with uncertainties in both axes. Trends Anal Chem 16:211–216. doi:10.1016/S0165-9936(97)00014-9
25. Mongomery DC (2000) Design and analysis of experiments, 3rd ed
26. Windig W, Guilment J (1991) Interactive self-modeling mixture analysis. Anal Chem 63:1425–1432. doi:10.1021/ac00014a016
27. Jaumot J, Tauler R (2010) MCR-BANDS: A user friendly MATLAB program for the evaluation of rotation ambiguities in Multivariate Curve Resolution. Chemom Intell Lab Syst 103:96–107. doi:10.1016/j.chemolab.2010.05.020
28. Gustavo González A, Ángeles Herrador M (2007) A practical guide to analytical method validation, including measurement uncertainty and accuracy profiles. Trends Anal Chem 26:227–238. doi:10.1016/j.trac.2007.01.009
29. Araujo P (2009) Key aspects of analytical method validation and linearity evaluation. J Chromatogr B 877:2224–2234. doi:10.1016/j.jchromb.2008.09.030
30. M. Mcloun JM, Forina M (1994) Chemometrics for Analytical Chemistry. In: Ellis Horwood C, West Sussex (ed). p 64
31. Gałuszka A, Migaszewski Z, Namieśnik J (2013) The 12 principles of green analytical chemistry and the SIGNIFICANCE mnemonic of green analytical practices. Trends Anal Chem 50:78–84. doi:10.1016/j.trac.2013.04.010
32. J. Inczédy TL, Ure AM, Gelencsér A, Hulanicki A (2000). In: Inc P (ed) Compendium of Analytical Nomenclature IUPAC, 3rd ed. p 50
33. Massart DL, Vandeginste, BGM, Buydens LMC, De Jong S, Lewi PJ, Smeyers-Verbeke J (1997) Handbook of Chemometrics and Qualimtrics: Part A. In: Elsevier (ed). pp 422–423
34. EURECHAM (2002) Guide to Quality in Analytical Chemistry. Prepared jointly by CITAC (The Cooperation on International Traceability in Analytical Chemistry) and Eurachem
35. Schmidt CK, Brouwer A, Nau H (2003) Chromatographic analysis of endogenous retinoids in tissues and serum. Anal Biochem 315:36–48. doi:10.1016/S0003-2697(02)00662-0
36. ICH International conference on harmonization of technical requirements for registration of pharmaceuticals for human use. Validation of analytical procedures: Text and methodology Q2 (R1)
37. EMEA (2012) EMEA/CHMP/EWP/192217/2009. Committee for Medicinal Products for Human Use (CHMP)
38. Ortiz MC, Sánchez MS, Sarabia LA (2009) 1.05 - Quality of Analytical Measurements: Univariate Regression. In: Brown SD, Tauler R, Walczak B (eds) Comprehensive Chemometrics. Elsevier, Oxford, pp 127–169. doi:10.1016/B978-044452701-1.00091-0